

Lu–H–N Phase Diagram from First-Principles Calculations

Fankai Xie(谢帆恺)^{1,2†}, Tenglong Lu(芦腾龙)^{1,2†}, Ze Yu(喻泽)^{1,2}, Yaxian Wang(王亚娴)¹,
Zongguo Wang(王宗国)³, Sheng Meng(孟胜)^{1,2,4*}, and Miao Liu(刘淼)^{1,4,5*}

¹Beijing National Laboratory for Condensed Matter Physics, Institute of Physics,
Chinese Academy of Sciences, Beijing 100190, China

²School of Physical Sciences, University of Chinese Academy of Sciences, Beijing 100190, China

³Computer Network Information Center, Chinese Academy of Sciences, Beijing 100083, China

⁴Songshan Lake Materials Laboratory, Dongguan 523808, China

⁵Center of Materials Science and Optoelectronics Engineering,
University of Chinese Academy of Sciences, Beijing 100049, China

(Received 21 March 2023; accepted manuscript online 31 March 2023)

Employing a comprehensive structure search and high-throughput first-principles calculation method on 1561 compounds, the present study reveals the phase diagram of Lu–H–N. In detail, the formation energy landscape of Lu–H–N is derived and utilized to assess the thermodynamic stability of each compound that is created via element substitution. The result indicates that there is no stable ternary structure in the Lu–H–N chemical system, however, metastable ternary structures, such as Lu₂₀H₂N₁₇ (*C2/m*) and Lu₂H₂N (*P3̄m1*), are observed to have small E_{hull} (< 100 meV/atom). It is also found that the energy convex hull of the Lu–H–N system shifts its shape when applying hydrostatic pressure up to 10 GPa, and the external pressure stabilizes a couple of binary phases such as LuN₉ and Lu₁₀H₂₁. Additionally, interstitial voids in LuH₂ are observed, which may explain the formation of Lu₁₀H₂₁ and LuH_{3- δ} N ϵ . To provide a basis for comparison, x-ray diffraction patterns and electronic structures of some compounds are also presented.

DOI: 10.1088/0256-307X/40/5/057401

Lu–H–N compounds have drawn increasing attention recently as it was reported that certain Lu–H–N phase exhibits appealing observable macroscopic quantum phenomenon at ambient condition, which may revolutionarily revolt the field of condensed matter physics. The existing literature^[1] has performed characterization and pointed out that the compound is the LuH_{3- δ} N ϵ in space group of *Fm3̄m* backed by the x-ray diffraction pattern, and doped with N. The synthesis process as they stated in the article is fairly accessible as the precursors are commercially available and experimental condition, such as pressure and temperature, is not critical by current technology. However, debate soars within the community as a group of scientists are skeptical about the results, hence extra experimental confirmations^[2] from multiple sources are demanded to settle down the arguments.^[3] This has set off a heat wave in the study of lutetium hydrogen systems recently.^[4-6] Fortunately, recent advances in high-throughput first-principles calculation along with large-scale database^[7-9] make it a feasible method to thoroughly search possible compounds within a certain chemical system, and accurately evaluate their likelihood of existence, way quicker than experimental approaches. In this Letter, we tackle the stability issue of possible phases in Lu–H–N chemical systems harnessing the high-throughput calculation and a large in-house database,^[10] which would hopefully provide useful knowledge for the community to un-

derstand the energy landscape of the Lu–H–N compounds.

From a scientific point of view, lanthanides hydrides are worth investigating as there are several high-temperature superconductors in this phase space under high pressure. For example, lanthanum decahydride (LaH₁₀) exhibits superconductivity under 252 K at the pressure of 170 GPa;^[11] yttrium-hydrogen (YH₉) exhibits superconductivity under 243 K at the pressure of 201 GPa.^[12] For Lu–H systems, recent experiments demonstrated that LuH₃ undergoes a phase transiting into the superconducting states at 12.4 K under 122 GPa.^[13] Meanwhile, it was found that the Lu₄H₂₃ exhibits superconductivity at 71 K under 218 GPa.^[14] However, the lanthanides hydrides are less explored compared to common metals, let alone the ternary compounds within the Lu–H–N chemical space. Given that it is alleged that a certain compound within the Lu–H–N chemical space possesses superconductivity at the very much near ambient condition,^[1] it is necessary to have a systematic search for viable structures within the Lu–H–N system.

Leveraging the recent advance in high-throughput first-principles calculation^[9,15-18] as well as the large trove of materials data,^[10] in this Letter, we closely investigate the possible compounds in the Lu–H–N chemical system. Such a method is fairly effective and has been demonstrated several times in searching for ternary nitrides,^[19] Kagome materials,^[20] superconductor,^[21] and many oth-

[†]These authors contributed equally to this work.

*Corresponding authors. Email: smeng@iphy.ac.cn; mliu@iphy.ac.cn

© 2023 Chinese Physical Society and IOP Publishing Ltd

ers, and more importantly, the theoretical predictions have been successfully confirmed by experiments.^[22,23] Essentially, we can use the existing compounds in a database as the structure templates and perform element substitution to create new structures within the targeting chemical systems, which is Lu–H–N in this case. Then the high-throughput first-principles calculations can optimize those structures and compute the energy of each compound. By comparing the formation energies of those compounds, the formation energy landscape can be obtained, and the thermodynamic stability of each compound can be derived to justify the likelihood of the existence of those compounds quantitatively.^[24]

Methodology. In thorough explanation, those compounds which boast the least formation energy, that is, the compounds that release the largest amount of enthalpy in their synthesis processes, are the ones that comprise the energy hull.^[24] This energy hull represents the boundary line of the maximum formation energy of a chemical structure. Therefore, the hull energy designates the lowest energy state potentially attainable by any feasible combination of elements capable of forming a compound with a given chemical composition. Upon this foundation, the energy disparity between a compound and the energy hull may furnish insight into the compound’s instability, or the “energy above the hull” (E_{hull}). E_{hull} conveys the minimum amount of energy required to break down the compound into the stable compounds present on the energy

convex hull.

In order to methodically assess the feasible compounds present in the Lu–H–N systems, initial 4478 structures are constructed by employing structural templates such as X–H–N, X–H–P, X–H–As, X–Li–N, X–Na–N, and X–K–N for ternary phases, and X–H, X–N, X–Li, and X–P for binary phases, resulting in 1561 newly created compounds after duplication removal. The computation is performed utilizing the Vienna ab initio simulation package (VASP)^[25–29] along with unified input parameters for Atomly.net. Further information with regard to the detailed input parameters could be found in Refs. [10,20,21,30]. All the structures and calculation results presented here can be found in Atomly.net materials database.

After conducting high-throughput calculations, totally 1561 structures are computed, including 712 Lu–H–N phases, 432 N–H phases, 116 Lu–H phases, and 301 Lu–N phases. The purpose of these calculations is to create a comprehensive “phase diagram” for Lu–H–N. Subsequently, we select all the compounds with relative stability and E_{hull} values less than 150 meV/atom. Those compounds are then calculated subjecting to hydrostatic pressure of up to 10 GPa with an interval of 1 GPa. Hence, the phase evolution of those compounds under pressure can be clearly captured and the phase diagrams under different pressured states are constructed and presented in this study.

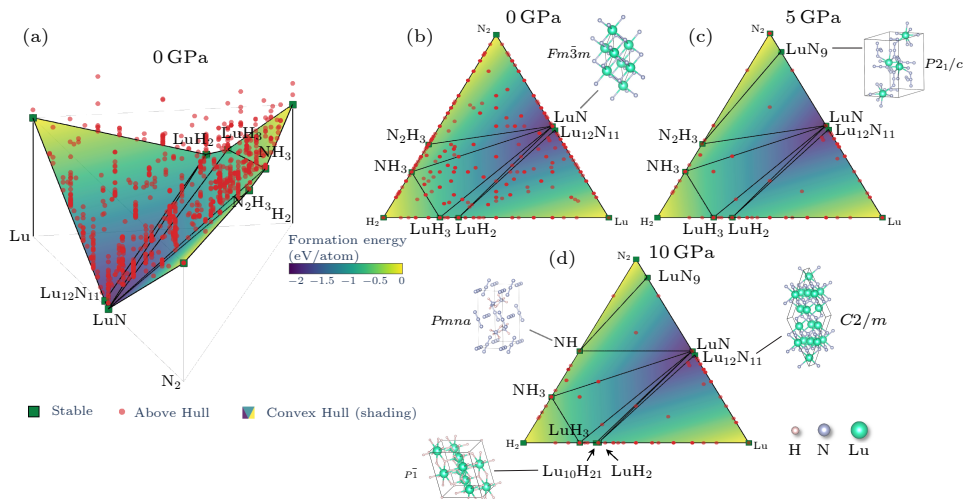


Fig. 1. Phase diagrams of Lu–H–N chemical system in both the 3D mode and 2D mode. The phase diagrams under 0 GPa, 5 GPa, and 10 GPa are calculated and presented to showcase the change of energy landscape as a function of hydrostatic pressure. On those plots, each data point shows a compound we calculate. Stable compounds are shown in green square dots, and unstable ones are shown in red circular dots. The energy convex hull is colored based on the formation energy.

Results and Discussions. Figure 1 presents the formation energy landscape of the Lu–H–N and its evolution versus external pressure. The phase diagram essentially presents that, at 0 GPa, there are six binary stable compounds, which are LuN ($Fm\bar{3}m$), Lu₁₂N₁₁ ($C2/m$), NH₃ ($Fm\bar{3}m$), N₂H₃ ($C2/c$), LuH₂ ($Fm\bar{3}m$),

and LuH₃ ($P\bar{3}c1$), and there is no stable Lu–H–N ternary phase. Among all the structures we have calculated, Lu₂₀H₂N₁₇ ($C2/m$), Lu₂H₂N ($P\bar{3}m1$), LuH₅N₂ ($P1$), Lu₃H₆N ($P2_1$), Lu₁₀HN₈ ($P\bar{1}$), Lu(H₁₅N₈)₂ ($P2_1/c$), Lu₆HN₆ (Cm), Lu₂H₅N (Pc), LuH₃N₂ ($P2_1/c$), LuH₅N ($P2_12_12_1$) are ternary metastable phases with small E_{hull}

(< 100 meV/atom), and the E_{hull} values are listed in Table 1. When pressure is applied, we spot some subtle changes in the phase diagram, for example, under 5 GPa, LuN₉ emerges as a stable phase, and under 10 GPa, Lu₁₀H₂₁ is

stabilized thermodynamically. There is no thermodynamic stable Lu–H–N ternary phase according to our evaluation under external pressure up to 10 GPa.

Table 1. List of some compounds with $E_{\text{hull}} < 100$ meV/atom at 0 GPa.^[10]

Composition	Space group	Atomly Id	E_{hull} (eV/atom)	Stability
Lu ₂₀ H ₂ N ₁₇	$C2/m$	1000313230	0.036	×
Lu ₁₀ HN ₈	$P\bar{1}$	1000313257	0.058	×
Lu(H ₁₅ N ₈) ₂	$P2_1/c$	1000313234	0.064	×
Lu ₆ HN ₆	Cm	1000313346	0.077	×
Lu ₂ H ₅ N	Pc	1000313150	0.081	×
Lu ₂ H ₂ N	$P\bar{3}m1$	1000313854	0.082	×
LuH ₃ N ₂	$P2_1/c$	1000313474	0.084	×
LuH ₅ N ₂	$P1$	1000313474	0.090	×
Lu ₃ H ₆ N	$P2_1$	1000313607	0.095	×
LuH ₅ N	$P2_12_12_1$	1000313153	0.099	×
NH ₃	$P2_13$	1000314459	0.000	✓
N ₂ H ₃	$C2/c$	1000314332	0.000	✓
LuH ₃	$P\bar{3}c1$	0000079762	0.000	✓
LuH ₂	$Fm\bar{3}m$	1000314722	0.000	✓
LuN	$Fm\bar{3}m$	3001350567	0.000	✓
Lu ₁₂ N ₁₁	$C2/m$	1000314893	0.000	✓

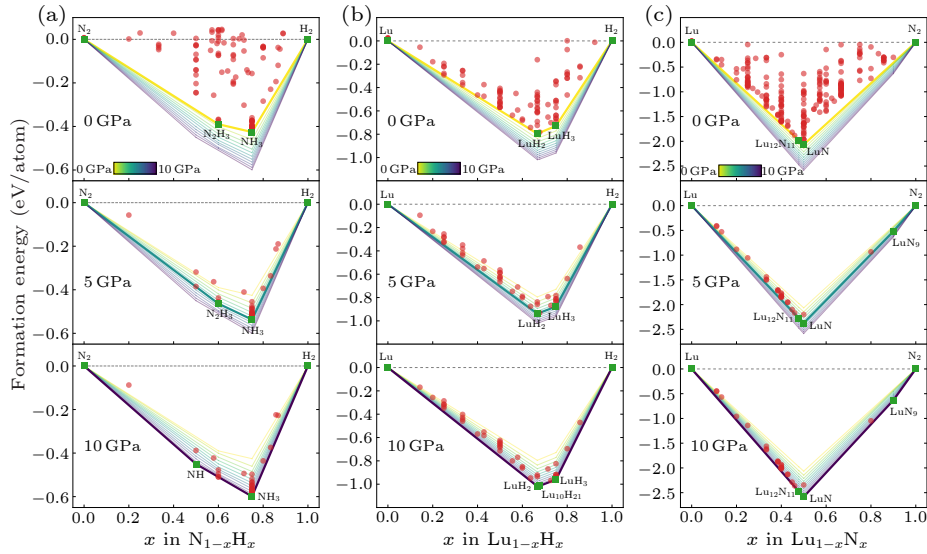


Fig. 2. N–H, Lu–H, and Lu–N binary phase diagrams under 0, 5, and 10 GPa separately. The compounds with $E_{\text{hull}} < 150$ meV/atom are selected to compute the formation energy under pressure > 0 GPa. (a) N–H phase diagram. NH becomes a stable phase under 10 GPa, while N₂H₃ becomes an unstable phase. (b) Lu–H phase diagram. Lu₁₀H₂₁ appears to become a new stable phase under the pressure of 10 GPa. (c) Lu–N phase diagram. With the increase of pressure, Lu could combine with more N. As there appears a new phase LuN₉ under the pressure of 5 GPa.

Figure 2 presents the phase evolution of binary compounds with or without external pressure. Clearly, the binary phase diagrams imply that the landscape of the Lu–H–N system is sensitive to pressure. For example, NH becomes stable when the pressure reaches 10 GPa. Many of the phases are not able to be found in other databases, evidencing that such a system has not been thoroughly investigated before. The existing databases including Materials Project,^[24,31,32] Aflow,^[16] and many others may miss the stable phases and thus are unable to extrapolate

the correct energy convex hull for this system. Except for the stable phases, the Lu–H phase diagram shows a group of compounds that have fairly low E_{hull} , such as Lu₁₀H₂₁, Lu₄H₇, Lu₃H₈, Lu₂H₃, Lu₃H₂, Lu₄H, and Lu₃H, implying that Lu and H are inter-mixable and can form many likely phases at different compositions. When 10 GPa pressure is applied, a new stable phase of Lu₁₀H₂₁ is observed to form. However, there is no new phase that contains a higher proportion of hydrogen than the original stable phase under 10 GPa.

The Lu–N phase diagram [Fig. 2(c)] suggests that LuN and Lu₁₂N₁₁ are the thermodynamic stable phases, and there are also several low E_{hull} compounds near Lu:N = 1:1 composition, such as Lu₂₀N₁₇, Lu₁₆N₁₃, and Lu₃N₂. Under 10 GPa, it is found that as the pressure increases, the formation energy of Lu–N decreases in comparison to its value at 0 GPa, indicating that the system becomes more stable. In addition, higher pressure can also result in the appearance of a new stable phase, LuN₉, suggesting that high pressure could facilitate forming of nitrogen-rich Lu–N compound.

Based on our calculation, it is generally difficult to form a Lu–H–N ternary compound as the LuH and LuN do not react with each other as there is no intermediate stable phase between LuN and LuH, and the lowest E_{hull} can be found from Lu₂HN and Lu₄HN₃, which are $E_{\text{hull}} = 168$ and 525 meV/atom, respectively. Both of them are too unstable to warrant the existence of those compounds. The reaction calculations give that when LuH and LuN are mixed, the most likely reaction is to form Lu₁₂N₁₁ and LuH₂ to reach the more stable phases. There are also no stable or relatively stable compounds within the *Immm* space group in Lu–H–N phases based on our evaluation with or without pressure.

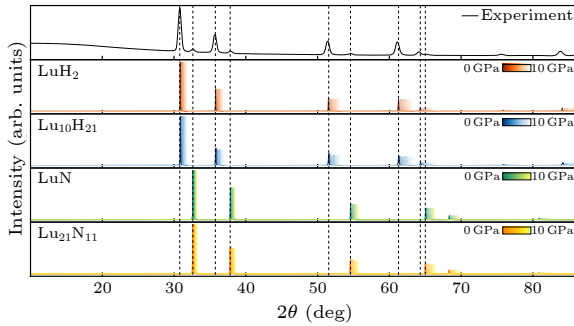


Fig. 3. The diffraction patterns of stable structures that matches the experimental XRD.^[1] Those compounds are LuH₂, Lu₁₀H₂₁, LuN, Lu₁₂N₁₁, in which Lu₁₀H₂₁ is basically the LuH₂ with addition interstitial H while Lu₁₂N₁₁ is LuN with N vacancy.

Figure 3 plots the compounds that share the same diffraction patterns as experimental observations among all the stable phases. Based on these patterns, it appears that LuH₂, Lu₁₀H₂₁, LuN, and Lu₁₂N₁₁ are likely to exist. Further investigation reveals that Lu₁₀H₂₁ is actually the same structure as LuH₂ but with H interstitials, and Lu₁₂N₁₁ is the same structure as LuN but with N vacancies. This suggests that increasing hydrostatic pressure may introduce H interstitials into LuH₂. At low doping concentrations, the H interstitials do not significantly change the volume of LuH₂ and may even contract the lattice parameter slightly. However, it is difficult to observe the Lu₁₀H₂₁ phase directly from the XRD as the volume of Lu₁₀H₂₁ is only 0.4% less than that of LuH₂. Similarly, the results suggest that N vacancies can be easily formed in LuN, as they are energetically favored and do not add too much strain energy. This may help to explain the experimental formation of LuH_{3- δ} N _{ϵ} with additional dopant, as the LuH₂ favors interstitial sites and can accommodate ex-

tra intercalants at low dopant concentration. When pressure is applied, the XRD peaks of LuH₂ shift drastically more than those in LuN, meaning that the LuN is elastically stiffer than LuH₂. Young’s moduli of LuH₂ and LuN from our calculation are 148.5 GPa and 338.1 GPa, respectively.

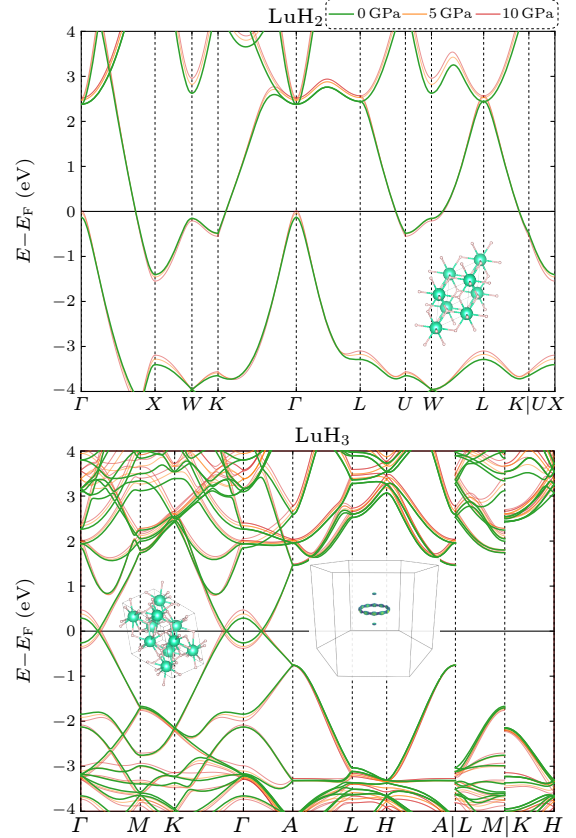


Fig. 4. Energy bands of LuH₂ ($Fm\bar{3}m$) and LuH₃ ($P\bar{3}c1$) under equilibrium and external pressure of 5 GPa and 10 GPa from first-principles calculation at the GGA-PBE level.

Figure 4 exhibits the calculated energy bands of LuH₂ ($Fm\bar{3}m$) and LuH₃ ($P\bar{3}c1$). Based on the energy band structures, LuH₂ is a metallic phase and the trigonal LuH₃ ($P\bar{3}c1$) can be classified into a node-line semimetal when spin-orbit coupling (soc) is not considered. As shown in Fig. 4, trigonal LuH₃ exhibits a clean electronic structure with an electron and hole pocket intersecting right at the Fermi level. Band inversion happens between $|Lu^+, d_{xz}/d_{yz}\rangle$ and $|H^{1-}, s\rangle$ and a nodal line is formed and protected by the glide-plane symmetry. The fact that the density of states is vanishing at the Fermi level makes LuH₃ an ideal system to study fundamental physics of topological node-line semimetals. With eliminated contributions of the topologically trivial bands, it is a unique platform to investigate manifestations of electron-hole interactions such as the linear frequency dependent optical conductivity^[33] and the hot carrier dynamics.^[34] Moreover, pressure-dependent band structure indicates that the nodal line is robust under hydrostatic pressure, yet it can serve as a manipulation of the Fermi velocity of the linearly

dispersed bands.

In summary, the recent advancement of high-throughput calculations has greatly improved the exploration and analysis of compound spaces with efficiency and accuracy. The focus of the present particular study focuses on investigating the different phases within the chemical space of Lu–H–N, resulting in the formation energy landscape. Hydrostatic pressure is also taken into consideration to simulate experimental conditions. It is found that there is no thermodynamic stable Lu–H–N ternary phase with or without external pressure up to 10 GPa. Lu₂₀H₂N₁₇ (*C2/m*), Lu₂H₂N (*P3m1*), LuH₅N₂ (*P1*), Lu₃H₆N (*P2₁*), Lu₁₀HN₈ (*P1̄*) are ternary phases with small E_{hull} (<100 meV/atom), hence they are the potential metastable ternary phases. Additionally, the binary phase diagram shows that Lu–H compounds are intermixable and may have various structures due to the numerous low E_{hull} Lu–H compounds calculated. The LuH₂ has interstitial sites, and thus can accommodate lightly doped intercalants, leading to the formation of Lu₁₀H₂₁ and N-doped LuH₂. The XRD compassion reveals that the experimental sample is likely to be composed of LuH₂ and LuN, and doped phases of them. Electronic structure analysis indicates that the LuH₂ is a metallic phase and LuH₃ is a nodal line semimetal. Overall, this work aims to provide valuable insights into the synthesizability of Lu–H–N compounds, and the developed algorithm can be further utilized to explore the vast territory of inorganic compounds and to accelerate the discovery of new materials.

Acknowledgment. This work was supported by Chinese Academy of Sciences (Grant Nos. CAS-WX2023SF-0101 and XDB33020000) and the National Key R&D Program of China (Grant Nos. 2021YFA1400200 and 2021YFA0718700). The computational resource is pro-

vided by the Platform for Data-Driven Computational Materials Discovery of the Songshan Lake laboratory.

References

- [1] Dasenbrock-Gammon N *et al.* 2023 *Nature* **615** 244
- [2] Ming X *et al.* 2023 arXiv:2303.08759 [cond-mat.supr-con]
- [3] Garisto D 2023 *Physics* **16**
- [4] Zhang S *et al.* 2023 arXiv:2303.11063 [cond-mat.supr-con]
- [5] Shan P *et al.* 2023 *Chin. Phys. Lett.* **40** 046101
- [6] Liu M *et al.* 2023 arXiv:2303.06554 [cond-mat.supr-con]
- [7] Zhou J *et al.* 2019 *Chem. Mater.* **31** 1860
- [8] Zhang T, Cai Z, and Chen S 2020 *ACS Appl. Mater. Interfaces* **12** 20680
- [9] Lu T *et al.* 2023 *Mater. Futures* **2** 015001
- [10] Website: <https://atomly.net>
- [11] Drozdov A *et al.* 2019 *Nature* **569** 528
- [12] Kong P *et al.* 2021 *Nat. Commun.* **12** 5075
- [13] Shao M *et al.* 2021 *Inorg. Chem.* **60** 15330
- [14] Li Z *et al.* 2023 arXiv:2303.05117 [cond-mat.supr-con]
- [15] Saal J E *et al.* 2013 *JOM* **65** 1501
- [16] Curtarolo S *et al.* 2012 *Comput. Mater. Sci.* **58** 218
- [17] Bo T *et al.* 2021 *J. Phys. Chem. Lett.* **12** 6667
- [18] Jia H *et al.* 2022 *Adv. Sci.* **9** e2202756
- [19] Sun W *et al.* 2019 *Nat. Mater.* **18** 732
- [20] Yu Z *et al.* 2022 *Phys. Rev. B* **105** 214517
- [21] Jiang Y *et al.* 2022 *Chin. Phys. Lett.* **39** 047402
- [22] Werhahn D *et al.* 2022 *Z. Naturforsch. B* **77** 757
- [23] Yang H *et al.* 2022 arXiv:2211.12264 [cond-mat.supr-con]
- [24] Ong S P *et al.* 2008 *Chem. Mater.* **20** 1798
- [25] Kresse G and Furthmüller J 1996 *Comput. Mater. Sci.* **6** 15
- [26] Kresse G and Furthmüller J 1996 *Phys. Rev. B* **54** 11169
- [27] Kresse G and Hafner J 1993 *Phys. Rev. B* **47** 558
- [28] Kresse G and Hafner J 1994 *J. Phys.: Condens. Matter* **6** 8245
- [29] Kresse G and Joubert D 1999 *Phys. Rev. B* **59** 1758
- [30] Liang Y *et al.* 2023 *Sci. Chin. Mater.* **66** 343
- [31] de Jong M *et al.* 2015 *Sci. Data* **2** 150009
- [32] Jain A *et al.* 2013 *APL Mater.* **1** 011002
- [33] Kirby R J, Scholes G D, and Schoop L M 2022 *J. Phys. Chem. Lett.* **13** 838
- [34] Johannsen J C *et al.* 2013 *Phys. Rev. Lett.* **111** 027403